Meccanica **31:** 421–432, 1996.

Cosserat and Cauchy Materials as Continuum Models of Brick Masonry

RENATO MASIANI and PATRIZIA TROVALUSCI
Università di Roma 'La Sapienza', Dipartimento di Ingegneria Strutturale e Geotecnica, Via A. Gramsci 53; 00197 Roma, Italy

(Received: 30 March 1995; accepted in revised form: 10 November 1995)

Abstract. Continuum modeling for masonry-like material accounting for bricks or blocks texture is discussed. The constitutive functions for the contact actions – expressed in terms of size, shape and arrangement of the block assembly – are derived within the framework of the linear elastic Cosserat and Cauchy theories. By varying some important geometrical parameters: the scale factor between the wall and the blocks size, the shape of the bricks and their arrangement, micropolar materials with particular internal constraints are obtained. In a few situations the constrained continuum behaves as a Cauchy continuum. In general, the Cauchy continuum does not provide a proper description of the brick masonry behaviour while the structured continuum model, accounting for the mutual blocks rotation, gives satisfactory results.

Sommario. Si studia la modellazione continua della muratura a blocchi, considerata come sistema discreto di corpi indeformabili, discutendo le proprietà di due continui equivalenti: un modello di Cosserat e uno di Cauchy. Nell'ambito della elasticità lineare, si forniscono le espressioni delle relazioni costitutive per le azioni di contatto, in funzione delle dimensioni, della forma e della disposizione dei mattoni. Modificando questi parametri geometrici si ottengono materiali equivalenti dotati di particolari vincoli interni. In alcuni rari casi il continuo di Cosserat vincolato si comporta come un continuo di Cauchy. Salvo queste eccezioni, il continuo classico è un modello inadeguato per la muratura a blocchi mentre un continuo dotato di struttura fornisce sempre risultati soddisfacenti.

Key words: Masonry, Macroscopic characterization, Continuum mechanics

1. Introduction

An important class of masonry structures is that made of bricks or stones properly assembled together in various regular dispositions. Since their mechanical behaviour is strongly influenced by the geometry, the arrangement and the orientation of the units, several authors have already attempted to develop models which take into account these features. Two approaches leading to micro and macro models are essentially proposed. One employs 'fine' descriptions based either on the continuum modeling of two distinct materials, the brick and the mortar, e.g. [1], [2], or on the discrete modeling of the actual discontinuous material as a multibody system [3], [4]. The other employs 'gross' continuum descriptions based either on the homogenization of masonry considered as a composite material with periodic structure [5]–[7], or on the direct identification from a discrete system of interacting blocks [8]–[10]. For systems with a large number of degrees of freedom the fine approach becomes inapplicable. For this reason, and because global results are often sufficient, it is advisable to resort to gross models, which roughly describe the discrete assembly, when practical problems are involved.

The proper selection of the equivalent continuum plays a crucial role. The simplest choice available is a Cauchy anisotropic continuum which gives satisfactory results for problems in which the relative rotations between the blocks are not relevant. It is easy to show that this model retains memory of the shape and the disposition of the blocks but not of their

dimensions. The mechanical behaviour is instead strongly influenced by the scale factor between the size of the elements and the relevant dimension of the body. For example, in the presence of loading or geometrical singularities – such as concentrated loads, openings and fractures – structures made of blocks of different size behave quite differently because the relative rotations between the bricks are involved, with effects depending on a 'length' parameter.

With regard to materials made of particles of finite dimensions which exhibit size effects, like concrete or granular materials, the idea of a microstructural continuum approach has already shown itself to be particularly appealing [11], [12]. The model with a micropolar structure differs from the classical one in some well known significant aspects which confirms its effectiveness with reference to these discrete frameworks. Firstly, the additional kinematical degree of freedom represented by the microrotation provides a natural way to describe the rotations of the single units [11], [13]. The mutual rotations between individual blocks, which play a crucial role, have the microrotation gradient as a continuum counterpart. Secondly, the stress tensor is not symmetric. This circumstance prevents some singularities from arising in the solution and allows the class of compatible boundary conditions to be widened [14], [15], [8]. Finally, the presence of the couple stresses allows the dimensions of the bricks to be included in the constitutive functions and thus to properly account for the size effects.

Some authors [8], [9] have already acknowledged that the Cauchy theory is not effective when the block dimensions are not small in comparison with the relevant dimensions of the body; therefore they adopted the Cosserat theory. While sharing this point of view, in this paper we also attempt to show that even when the size of the units is small, contrary to common expectations, a structured continuum description is required. The classical continuum is suitable only in a few cases, lacking practical interest: when the disposition of the units is strongly symmetric and their size is negligible. The above considerations and the tolerable complexity of the model confirm the choice of a Cosserat material as an effective model for block masonry.

2. Identification of the Equivalent Continua

The constitutive relations for the contact actions, the body forces and the surface forces of the equivalent micropolar continuum can be identified employing the procedure presented, with all the details, by Masiani *et al.* [10].

First we consider the masonry as a discrete system made of rigid blocks interacting two by two through the contact surfaces. The rigid displacement of a generic point of a block $\mathcal{A}$ is described, within the framework of a linearized theory, by means of the displacement of the centre of mass $\mathbf{w}(g^a) \in V$ and the rotation of the block $\mathbf{W}^a \in \mathrm{Skw}$ (cf. Equations (17) in [10]).[1] For each pair of adjacent blocks $\mathcal{A}$ and $\mathcal{B}$, we define two linearized strain measures: the relative displacement $\mathbf{w}_p = \mathbf{w}(p^b) - \mathbf{w}(p^a)$ between two material points ('test pair') belonging to $\mathcal{A}$ and $\mathcal{B}$, whose positions in the reference shape are p^a and p^b, and the relative rotation $\mathbf{W}_p = \mathbf{W}^b - \mathbf{W}^a$ between the two blocks.

The contact actions that $\mathcal{B}$ exerts on $\mathcal{A}$ are described by a class of equivalence represented by the force $\mathbf{t}_p \in V$ applied at p^a and by the couple $\mathbf{C}_p \in \mathrm{Skw}$. The actions on $\mathcal{B}$ are obtained from balance.

[1] Sym and Skw are, respectively, the sets of the symmetric and skew-symmetric elements of the set Lin of the linear transforms of the vector space V into itself.

Then we establish a correspondence between the motion of a part $\mathcal{P}$ of the block assembly and that of a neighbourhood of a continuum with micropolar structure. We assume that the motion of the part $\mathcal{P}$ is smooth so that the discrete fields of the displacement $\mathbf{w}(g^a)$ and the rotation $\mathbf{W}^a$ admit a local representation as

$$\mathbf{w}(g^a) = \mathbf{u}(x) + \mathbf{H}(x)(g^a - x), \qquad \mathbf{W}^a = \mathbf{R}(x) + \mathsf{H}(x)(g^a - x) \tag{1}$$

where $\mathbf{u}(x)$ and $\mathbf{R}(x) \in \mathrm{Skw}$ are respectively the linearized displacement and microrotation fields of the continuum, $\mathbf{H} = \mathrm{grad}(\mathbf{u}) \in \mathrm{Lin}$ and $\mathsf{H} = \mathrm{grad}(\mathbf{R}) \in \mathrm{LIN}$.[2] Hence, the strain measures for the test pair (p^a, p^b) can be expressed in terms of continuum strain measures $\mathbf{H} - \mathbf{R}$ and H (Equations (25) in [10]).

In order to identify the stress measures of the equivalent continuum, represented by the stress tensor $\mathbf{S} \in \mathrm{Lin}$ and the couple-stress tensor $\mathsf{S} \in \mathrm{LIN}$, we finally assume that the density of mechanical power expended by the contact actions in $\mathcal{P}$ (Equation (22) in [10]) and in the continuum medium (Equation (14) in [10]) is the same for any admissible velocity field $\dot{\mathbf{H}} - \dot{\mathbf{R}}$, $\dot{\mathsf{H}}$. This is true if and only if the continuum contact actions admit the following expressions

$$\begin{aligned}
\mathbf{S}(x) &= \frac{1}{\mathrm{vol}\,\mathcal{P}} \sum_p \mathbf{t}_p \otimes (g^b - g^a), \\
\mathsf{S}(x) &= \frac{1}{\mathrm{vol}\,\mathcal{P}} \sum_p \{\, 2\mathbf{t}_p \otimes [(p^b - g^b) \otimes (g^b - x) - (p^a - g^a) \otimes (g^a - x)] \\
&\quad + \mathbf{C}_p \otimes (g^b - g^a) \,\}
\end{aligned} \tag{2}$$

functions of the mechanical actions between the bricks and their geometrical fabric.

To make a comparison we also identify the contact actions of a Cauchy continuum applying the same equivalence procedure. Let us establish a correspondence between the motion of the part $\mathcal{P}$ of the block assembly and of a neighbourhood of a Cauchy body in such a way that

$$\mathbf{w}(g^a) = \mathbf{u}(x) + \mathbf{H}(x)(g^a - x), \qquad \mathbf{W}^a = \mathrm{skw}\mathbf{H}(x). \tag{3}$$

With these hypotheses, the strain measures of the discrete can be written as

$$\mathbf{w}_p = \mathrm{sym}\mathbf{H}(x)(g^b - g^a), \qquad \mathbf{W}_p = \mathbf{0}. \tag{4}$$

As above, by equating the mechanical virtual power density of the fine and the gross model – both expressed in terms of the continuum strain measure $\mathrm{sym}\mathbf{H}$ – we can identify the expression for the Cauchy stress tensor $\check{\mathbf{S}}$ in terms of the contact forces and geometrical parameters of the discrete

$$\check{\mathbf{S}}(x) = \frac{1}{\mathrm{vol}\,\mathcal{P}} \sum_p \mathrm{sym}(\mathbf{t}_p \otimes (g^b - g^a)). \tag{5}$$

3. Constitutive Functions for the Contact Actions

The procedure of power equivalence allows the correspondence between the continuum and the discrete contact actions to be determined without declaring the nature of their response

[2] $\mathrm{LIN} := V \to \mathrm{Skw}$.

function. We assume below that the interactions between the bricks are linear elastic and vanish in the reference configuration, therefore we write[3]

$$\mathbf{t}_p = \mathbf{K}(p)\mathbf{w}_p, \qquad \mathbf{C}_p = \mathbb{K}(p)\mathbf{W}_p. \tag{6}$$

Assuming the representation (1) for the displacements of the discrete, the expressions (6) can be written in terms of continuum strain measures and then substituted into Equations (2). After some algebra, we obtain the linear relations between the stress and the local strain measures of the structured continuum in the form[4]

$$\begin{aligned} \mathbf{S}(x) &= \mathbb{A}(x)[\mathbf{H}(x) - \mathbf{R}(x)] + \mathbb{B}(x)[\mathsf{H}(x)], \\ \mathsf{S}(x) &= \mathbb{C}(x)[\mathbf{H}(x) - \mathbf{R}(x)] + \mathbb{D}(x)[\mathsf{H}(x)]. \end{aligned} \tag{7}$$

Likewise, if the discrete strain measures are described by Equations(4), from Equations (5) and (6) we derive the constitutive expressions for the contact actions of the Cauchy equivalent material in the form

$$\check{\mathbf{S}}(x) = \check{\mathbb{A}}(x)[\mathrm{sym}\,\mathbf{H}(x)]. \tag{8}$$

The components of the elasticity tensors $\mathbb{A}, \mathbb{B}, \mathbb{C}$ and $\mathbb{D}$, in the Cosserat frame, and $\check{\mathbb{A}}$, in the Cauchy frame, are expressed in terms of the geometry of the blocks and of the elastic constants of the contacts. Here we assume that the tensors $\mathbf{K}(p)$ and $\mathbb{K}(p)$ are symmetric, [5] consequently we have $\mathbf{U}\cdot\mathbb{A}\mathbf{V} = \mathbf{V}\cdot\mathbb{A}\mathbf{U}$, $\mathsf{U}\cdot\mathbb{D}\mathsf{V} = \mathsf{V}\cdot\mathbb{D}\mathsf{U}$, $\mathbb{B}\mathsf{U}\cdot\mathbf{U} = \mathsf{U}\cdot\mathbb{C}\mathbf{U}$, $\forall\mathbf{U},\mathbf{V}\in\mathsf{Lin}$ and $\forall\mathsf{U},\mathsf{V}\in\mathsf{LIN}$, and the material results as being hyperelastic.

In order to define the symmetry groups for the equivalent materials, we introduce the following groups[6]

$$\begin{aligned} \mathcal{G}_{\mathbb{A}} &:= \{\mathbf{Q}\in\mathsf{SO(3)}\,|\mathbf{Q}*\mathbb{A}[\mathbf{U}] = \mathbb{A}[\mathbf{Q}*\mathbf{U}], \forall\mathbf{U}\in\mathsf{Lin}\}, \\ \mathcal{G}_{\mathbb{B}} &:= \{\mathbf{Q}\in\mathsf{SO(3)}\,|\mathbf{Q}*\mathbb{B}[\mathsf{U}] = \mathbb{B}[\mathbf{Q}*\mathsf{U}], \forall\mathsf{U}\in\mathsf{LIN}\}, \\ \mathcal{G}_{\mathbb{C}} &:= \{\mathbf{Q}\in\mathsf{SO(3)}\,|\mathbf{Q}*\mathbb{C}[\mathbf{U}] = \mathbb{C}[\mathbf{Q}*\mathbf{U}], \forall\mathbf{U}\in\mathsf{Lin}\} \\ \mathcal{G}_{\mathbb{D}} &:= \{\mathbf{Q}\in\mathsf{SO(3)}\,|\mathbf{Q}*\mathbb{D}[\mathsf{U}] = \mathbb{D}[\mathbf{Q}*\mathsf{U}], \forall\mathsf{U}\in\mathsf{LIN}\}, \\ \mathcal{G}_{\check{\mathbb{A}}} &:= \{\mathbf{Q}\in\mathsf{SO(3)}\,|\mathbf{Q}*\check{\mathbb{A}}[\mathbf{U}] = \check{\mathbb{A}}[\mathbf{Q}*\mathbf{U}], \forall\mathbf{U}\in\mathsf{Sym}\}, \end{aligned} \tag{9}$$

where the asterisk indicates the action of the group on a tensor.[7] The symmetry group for the Cosserat material is $\mathcal{G} := \mathcal{G}_{\mathbb{A}}\cap\mathcal{G}_{\mathbb{B}}\cap\mathcal{G}_{\mathbb{D}}$;[8] for the Cauchy material the symmetry group is $\mathcal{G}_{\check{\mathbb{A}}}$.

In the right hand side of expressions (2) the variable x appears explicitly, but also the functions $\mathrm{vol}\,\mathcal{P}$ and '$\sum_p$' depend on x. If the bricks assembly has a periodic structure, a 'module' can be defined as the smallest volume element accounting for all kinds of dynamical interaction between the bricks. Choosing such a module as part $\mathcal{P}$, the equivalent continuum results in being homogeneous. If the assembly is non-periodic, the procedure can still be applied by obtaining a non-homogeneous equivalent continuous material; the identification

[3] $\mathbf{K} := \mathsf{V}\to\mathsf{V}$; $\mathbb{K} := \mathsf{Skw}\to\mathsf{Skw}$.

[4] $\mathbb{A} := \mathsf{Lin}\to\mathsf{Lin}$; $\mathbb{B} := \mathsf{LIN}\to\mathsf{Lin}$; $\mathbb{C} : \mathsf{Lin}\to\mathsf{LIN}$; $\mathbb{D} := \mathsf{LIN}\to\mathsf{LIN}$.

[5] That is $\mathbf{u}\cdot\mathbf{K}\mathbf{v} = \mathbf{v}\cdot\mathbf{K}\mathbf{u}$, $\forall\mathbf{u},\mathbf{v}\in\mathsf{V}$ and $\mathbf{U}\cdot\mathbb{K}\mathbf{V} = \mathbf{V}\cdot\mathbb{K}\mathbf{U}$, $\forall\mathbf{U},\mathbf{V}\in\mathsf{Skw}$.

[6] SO(3) is the group of the proper orthogonal transformation of the 3-D euclidean space.

[7] In terms of components, the action of an element $\mathbf{Q}$ of the group on a tensor $\mathbb{T}$ yields $(\mathbf{Q}*\mathbb{T})_{ij\ldots m} = \mathbb{T}_{ab\ldots n}\mathbf{Q}_{ia}\mathbf{Q}_{jb}\cdots\mathbf{Q}_{mn}$. With $\mathbb{T}_{ij\ldots m} = \mathbb{T}\cdot\mathbf{e}_i\otimes\mathbf{e}_j\otimes\cdots\otimes\mathbf{e}_m$.

[8] For hyperelastic materials $\mathcal{G}_{\mathbb{C}}\equiv\mathcal{G}_{\mathbb{B}}$.

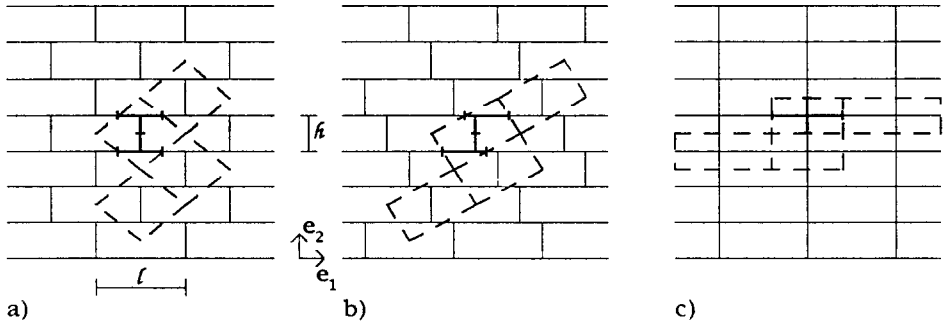

Figure 1. Examples of masonry textures and corresponding moduli

will be carried out point by point assuming an arbitrary neighborhood as part $\mathcal{P}$ on which to establish the power equivalence. In both cases, the part of the discrete framework must be small in order to satisfy the hypothesis of regularity on the motions implicit in Equations (1) and (3).

Henceforth we focus our attention on 2-D walls with periodic textures. In Figure 1 two examples of ordinary periodic bricks textures are sketched along with an unusual but significant case. Since the continuum constitutive functions are directly related to the geometry of the module, and in particular to the arrangement of the units, by changing the disposition of the bricks the continuum elastic coefficients, and the classification in terms of material symmetries, are modified. We define symmetric transformations for the discrete medium as being the rotations of the module which leave unchanged the power expended in any admissible displacement field. It can be shown that the symmetric transformations of the structured continuous material correspond to those of the discrete material [16]. This is an essential requirement for a gross equivalent model not always satisfied by the Cauchy model. For example,[9] choosing the orthonormal base $\{\mathbf{e}_i\}$ $(i = 1, 3)$ shown in Figure 1, the modules (a) and (c) are symmetric with respect to the rotations of amplitude π about the two axis $\mathbf{e}_1$, $\mathbf{e}_2$: $\mathbf{Q}_1^\pi = 2\mathbf{e}_1 \otimes \mathbf{e}_1 - \mathbf{I}$ and $\mathbf{Q}_2^\pi = 2\mathbf{e}_2 \otimes \mathbf{e}_2 - \mathbf{I}$. Both the micropolar and the classic equivalent materials are orthotropic materials whose symmetry groups are generated by $\mathbf{Q}_1^\pi$ and $\mathbf{Q}_2^\pi = 2\mathbf{e}_2 \otimes \mathbf{e}_2 - \mathbf{I}$.[10] For the module (b) the symmetric transformations are generated by $\mathbf{Q}_3^\pi$. This rotation also generates the symmetry group of the Cosserat material, while the Cauchy material is orthotropic. Finally, if the texture (c) consists of square blocks, the discrete and both the continuous materials have the so-called ortho-tetragonal symmetry. In this case, the symmetry group generators are $\mathbf{Q}_1^\pi$ and $\mathbf{Q}_3^{\pi/2} = \mathbf{e}_3 \otimes \mathbf{e}_3 + \mathbf{e}_2 \otimes \mathbf{e}_1 - \mathbf{e}_1 \otimes \mathbf{e}_2$.

4. Size and Shape Effects

To analyze the influence of the geometry of the blocks we express the components of the elasticity tensors $\mathbb{A}$, $\mathbb{D}$ and $\check{\mathbb{A}}$ in terms of the two dimensionless parameters ρ and ε. With reference to the Cosserat continuum, if $\mathbf{Q}_3^\pi \in \mathcal{G}$, as for the three cases considered, the tensors $\mathbb{B}$ and $\mathbb{C}$ are the null tensors. The parameter ρ $(\rho > 0)$, here called 'aspect ratio', is the ratio between the length l and the height h of the block. The ratio ε $(0 < \varepsilon \leq 1)$ between the block length and a characteristic length of the body, for example the width of the panel, is a 'scale factor' which relates the dimension of the geometric micro-structure to the macroscopic one.

[9] We assumed here that the tensor fields $\mathbf{K}(p)$ and $\mathbb{K}(p)$ do not alter the geometrical symmetry of the module.

[10] These groups also contain the rotation $\mathbf{Q}_3^\pi$ since $\mathbf{Q}_1^\pi \circ \mathbf{Q}_2^\pi = 2\mathbf{e}_3 \otimes \mathbf{e}_3 - \mathbf{I}$.

Table 1. Constitutive terms for the modules of Figure 1, as functions of the parameters ε and ρ.

	Cosserat		Cauchy
$\mathbb{A}_{1111}$	$b_1 k_n \rho + b_2 k_t \rho^2$	$\check{\mathbb{A}}_{1111}$	$b_1 k_n \rho + b_2 k_t \rho^2$
$\mathbb{A}_{2222}$	$b_1 k_n$	$\check{\mathbb{A}}_{2222}$	$b_1 k_n$
$\mathbb{A}_{1212}$	$b_1 k_t$	$\check{\mathbb{A}}_{1212}$	$\frac{1}{2}(b_1 k_t(1+\rho) + b_2 k_n \rho^2)$
$\mathbb{A}_{2121}$	$b_1 k_t \rho + b_2 k_n \rho^2$		
$\mathbb{D}_{121121}$	$(b_3 k_n \rho^{-1} + b_4 k_n \rho^2 + b_5 k_t)\varepsilon^2$		
$\mathbb{D}_{122122}$	$(b_6 k_n + b_7 k_t \rho^{-2} + b_8 k_t \rho^{-1})\varepsilon^2$		
$\mathbb{D}_{121122}$	$(b_9 k_n + b_{10} k_t)\varepsilon^2 \rho$		

The elastic coefficients as functions of the parameters ε and ρ are obtained by assuming the following hypothesis for the discrete framework. Two independent sets of linear elastic springs, respectively acting in the direction normal and tangential to the joint, describe the link between two bricks. The independence between the two layers of springs accounts for the absence of dilatancy in the joints. The thickness of the head joints (normal to $\mathbf{e}_1$) is assumed equal to that of the bed joints (normal to $\mathbf{e}_2$) and proportional to the height of the bricks with a factor η. As a result, the non zero components of $\mathbf{K}$ and $\mathbb{K}$ in Equation (6) for each test pair along the head joints are: $\mathbf{K}_{11} = a_1 \eta k_n$, $\mathbf{K}_{22} = a_1 \eta k_t$; $k_r = a_2 \eta k_n \varepsilon^2 \rho^{-2}$ and for the test pairs along the bed joints: $\mathbf{K}_{11} = a_3 \eta \rho k_n$, $\mathbf{K}_{22} = a_3 \eta \rho k_t$; $k_r = a_4 \eta k_n \varepsilon^2 \rho$. Here k_n and k_t are respectively the normal and the tangential stiffness per unit length and unit thickness of the joint, $k_r = \mathbb{K}_{1212} - \mathbb{K}_{1221} = \mathbb{K}_{2112} - \mathbb{K}_{2121}$ is the sole independent component of the tensor $\mathbb{K}$ in 2-D and a_i are constants depending on the disposition of the bricks.

In Table 1 the non zero components of the Cosserat and the Cauchy elasticity tensors common to the three patterns of Figure 1 are represented.

As a consequence of the hypothesis $\mathbf{K}_{12} = \mathbf{K}_{21} = 0$ and due to the symmetries of the modules examined, the elasticity tensors $\mathbb{A}$ and $\check{\mathbb{A}}$ result in being diagonal. Moreover, the Young's moduli of the Cauchy material are equal to those of the micropolar material, while the classical shear modulus is equal to the mean value of the two Cosserat shear moduli. The constants b_i depend on the arrangement of the units. In particular: $b_8 = b_9 = b_{10} = 0$ for the module (a), $b_8 = 0$ for (b) and $b_2 = b_4 = b_7 = b_9 = b_{10} = 0$, $b_3 = b_5 = b_6 = b_8$ for (c).

Note that the components of both the tensors $\mathbb{A}$ and $\check{\mathbb{A}}$ do not depend on the size of the blocks (ε) but only on their shape (ρ). On the contrary, the couple-stresses depend on the size of the bricks besides of their shape. This property is a fundamental characteristic of the micropolar materials. Conversely, the classical continuum, lacking the microrotation kinematical descriptors and their dynamical counterparts, cannot account for the difference between small and large blocks.

To clarify the predicting possibilities provided by the micropolar model and, in particular, to know for which conditions the equivalent continuum behaves as a classical Cauchy material, we study the cases in which the area of the bricks approaches zero by acting on the geometrical parameters ρ and ε. It can be shown that different assumptions for the discrete model – for instance different thicknesses between the head and bed joints – lead qualitatively to the same asymptotic results. Three situations will be studied in detail. Two of them afford particular constitutive prescriptions for the material, which can be interpreted as internal constraints.

Case C1. $\varepsilon \to 0$, constant ρ. With respect to the dimensions of the wall, the width and the height of the brick vanishes at the same rate. This is the case of a panel made of a large number of small bricks. The components of $\mathbb{A}$ and of $\check{\mathbb{A}}$ remain unchanged. Instead, all the drilling stiffness coefficients of $\mathbb{D}$ approach zero as ε^2; this leads to the constitutive prescription for the micropolar continuum that the couple-stress field vanishes whatever is the microrotation gradient

$$\mathsf{S} = 0. \tag{10}$$

The stress tensor is, in general, asymmetric and its skew-symmetric part can be evaluated directly from the moment balance Equation (13b) in [10] that, in terms of strain components, becomes

$$(\mathbb{A}_{1212} - \mathbb{A}_{2121})\tfrac{1}{2}(\mathbf{H}_{12} + \mathbf{H}_{21}) - (\mathbb{A}_{1212} + \mathbb{A}_{2121})(\tfrac{1}{2}(\mathbf{H}_{12} - \mathbf{H}_{21}) - \mathbf{R}_{12}) = \mathbf{B}_{12} \tag{11}$$

where $\mathbf{B} \in Skw$ is the body couple density. This equation has an interesting consequence when the two elastic coefficients $\mathbb{A}_{1212}$ and $\mathbb{A}_{2121}$ – which relate the angular distortions to the corresponding tangential stresses – are equal. This occurs if the material symmetry group contains the rotation $\mathbf{Q}_3^{\pi/2}$. For $\mathbf{B} = \mathbf{0}$, the moment balance affords the internal constraint between the displacement gradient and the microrotation field

$$\operatorname{skw} \mathbf{H} - \mathbf{R} = \mathbf{0} \tag{12}$$

In the Appendix we show that a Cosserat material with the constitutive prescriptions (10) and (12) behaves, in the absence of body couples, like a Cauchy material and has $\check{\mathbb{A}}$ as elasticity tensor. Instead, restraining the Cosserat solution only by Equation (10) we obtain the solution of a particular structured continuum here called 'reduced Cosserat'. The structured equivalent continuum behaves as the classical equivalent continuum only if the size of the brick approaches zero and the module has at least ortho-tetragonal symmetry. For instance, as in the case of walls made of square bricks arranged in a texture of the kind (c), unusual in constructive practice.

The next two situations are interesting in order to clarify the influence of the aspect ratio when only one of the dimensions of the blocks approaches zero and the dimensions of the wall remain unchanged. If one decreases the length of the brick or its height the effects on the equivalent materials are very different.

Case C2. $\rho \to \infty$, constant ε. The brick's height vanishes while its width is fixed. Some of the terms in the constitutive relations, relative to both the stress and the couple-stress components, become singular. As it is necessary that the strain energy be bounded, the strain measures corresponding to boundless stress measure must be constrained to zero. The continuum obtained can be interpreted as a partially constrained continuum within the meaning specified in [17]. For example, with reference to the module (a) the constraints are $(\mathbf{H} - \mathbf{R})\mathbf{e}_1 = \mathbf{0}$, $\mathsf{H}\mathbf{e}_1 = \mathbf{0}$ in the Cosserat case, and $\operatorname{sym} \mathbf{H}\mathbf{e}_1 = \mathbf{0}$, in the Cauchy case. Note the difference between the micropolar and the classical model: the Cosserat model retains the possibility to exhibit one non zero component of angular distortion; instead, in the Cauchy model a reduction of the height of the blocks leads to a complete shear nondeformability.

Case C3. $\rho \to 0$, constant ε/ρ. The length of the brick vanishes with fixed height. In this situation only the stress $\mathbf{S}\mathbf{e}_2$, and $\mathsf{S}\mathbf{e}_2$ are different from zero, no terms become singular and no kinematical constraints are needed. From a physical point of view, the vanishing of some

drilling stiffness accounts for the loss of interlocking between the bricks due to the shortening of their length.

5. Numerical Comparisons

To evaluate the effectiveness of the proposed continuum models, we have solved numerically one test problem comparing three different solutions. The first one is the discrete model of the assembly of rigid bodies with linear elastic contacts: we assume its results as the 'actual' behaviour of the masonry. The second one is the Cosserat continuum equivalent model: we have solved the field problem by a finite element discretization, using a three nodes triangular element with three degrees of freedom per node: two displacements and one in-plane rotation, with linear shape functions. Thirdly, we have tested the Cauchy continuum equivalent model, using the same discretization as in the previous case with the proper modifications.

The test problem is a square panel whose dimensions are 800×800, with the bricks disposed as texture (a) in Figure 1, with $\varepsilon = 1/10$ and $\rho = 4$, that is $l = 80$ and $h = 20$. The panel was subject to a concentrated contact force, of components $f_1 = 0$ and $f_2 = 2 \times 10^2$, applied in the middle of the top side. As constitutive constants of the joints in the discrete we assumed $k_n = 1.25 \times 10^5 \rho^{-1}$, $k_t = 2.50 \times 10^4$, $\eta = 0.20$, $a_1 = 1.00$, $a_2 = 5.33 \times 10^4$, $a_3 = 0.25$, $a_4 = 3.33 \times 10^3$.

In Figure 2 the contour lines of the components of the fields of displacement and rotation for the discrete problem are compared to the corresponding values of the Cosserat and Cauchy solution. Further results, in terms of the components of strain measures, are shown in Figure 3. The displacement gradient of the discrete solution has been evaluated by means of the finite difference technique.

Note that, because of the diagonal constitutive relations of the continuum, all the strain measures are proportional to the corresponding stress measures. Resorting to the symmetry of the problem, we divided each plot into two parts representing on the left side the results of the discrete model and on the right side the results of the continuum solutions. The Cosserat solution is consistent with the discrete solution both in qualitative and, particularly, in quantitative terms. Due to the effects of the couple-stress the diffusion of the vertical forces, caused by the interlocking among the blocks in the discrete framework, is well reproduced by the Cosserat material.

To numerically investigate the influence of the scale factor we also modified the length of the bricks. The comparison is made with reference to a global response parameter, here the work of the external forces. The diagram in Figure 4 (a) shows the results obtained for $\rho = 4$ by changing the value of ε. Three curves are plotted relative to the Cosserat, the Cauchy and the reduced Cosserat solutions. The results obtained by the Cosserat model are very close to the actual ones indicated by block squares. Although there is an appreciable correspondence for values of the scale factor corresponding to the ordinary masonry walls ($\varepsilon = 1/25, 1/15$), the approximation is more satisfactory for smaller ε, i. e. for small blocks. The discrete and the micropolar solutions move asymptotically towards the result of the reduced Cosserat material, that represents the limit solution for blocks of negligible dimensions. Instead, the Cauchy model gives a response independent from ε, as stated in the previous sections, not corresponding to the discrete solution and apparently without a clear physical meaning.

In Figure 4 (b) the results of the same problem in terms of the aspect ratio ρ are represented, assuming $\varepsilon = 1/20$. The Cauchy equivalent material is able to account for the shape of the bricks. However, its consistency with the actual solution depends on the value of ε and

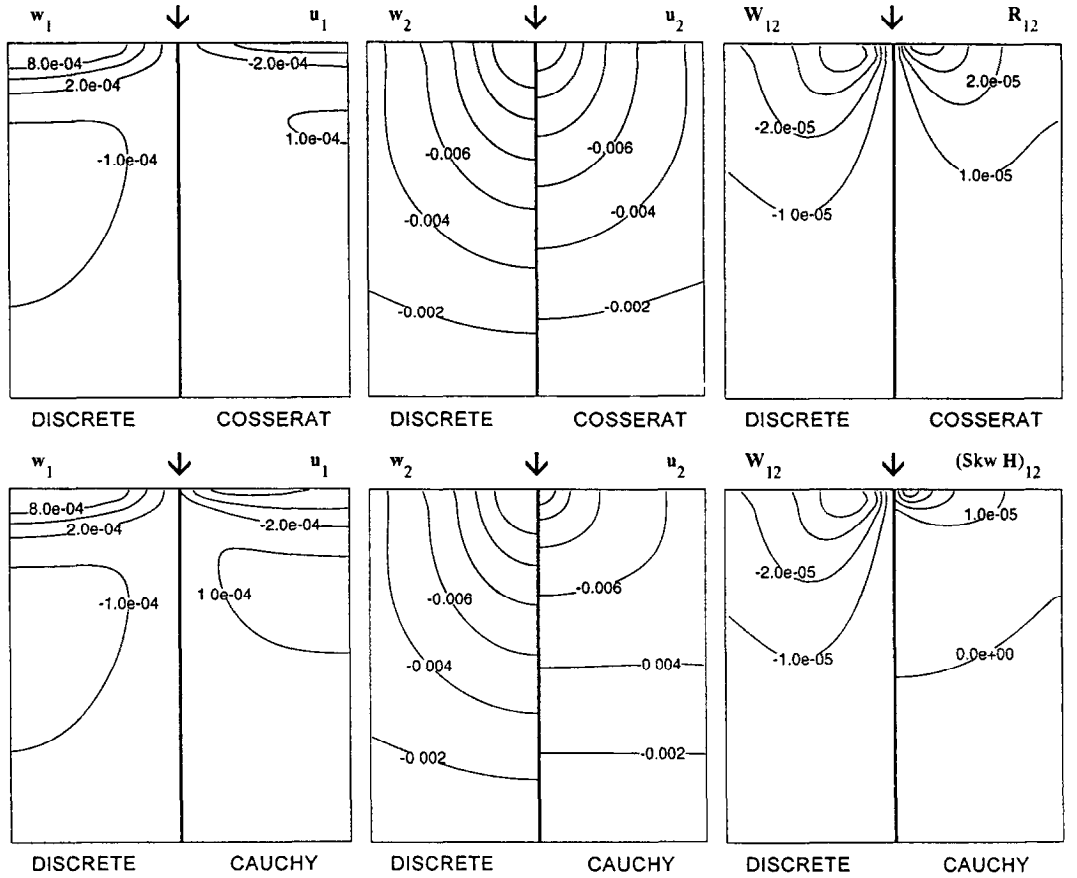

Figure 2. Contour lines of the components of the displacement $\mathbf{w}$ and rotation $\mathbf{W}$ of the blocks, compared to the displacement $\mathbf{u}$ and microrotation $\mathbf{R}_{12}$ (Cosserat) or infinitesimal rigid rotation $1/2(\mathbf{H}_{12} - \mathbf{H}_{21})$ (Cauchy).

may prove ineffective in different situations, while the micropolar material always gives satisfactory results.

6. Concluding Remarks

The usefulness of a continuum model for the brick masonry is evident whenever a fine description of the masonry proves to be impracticable or unnecessary. Whichever is the type of equivalent material, the proposed identification procedure affords a simple way to obtain directly all the constitutive parameters from the mechanical and the geometrical properties of the discrete. Nevertheless, since experimental tests show that for many problems the dimensions of the units, as well as their arrangement and their orientation, strongly affect the mechanical behaviour of block masonry, a gross modeling of the masonry must take into account the size effects.

Accordingly, the main issue of the paper lies in two considerations, concerning the nature of the equivalent continuum. First of all, a micropolar continuum is able to account for the size effects of the masonry, while the Cauchy model implicitly requires that the scale factor be zero. Secondly, even if the dimensions of the bricks are small, the Cosserat equivalent continuum behaves as the classical continuum only for textures corresponding to ortho-

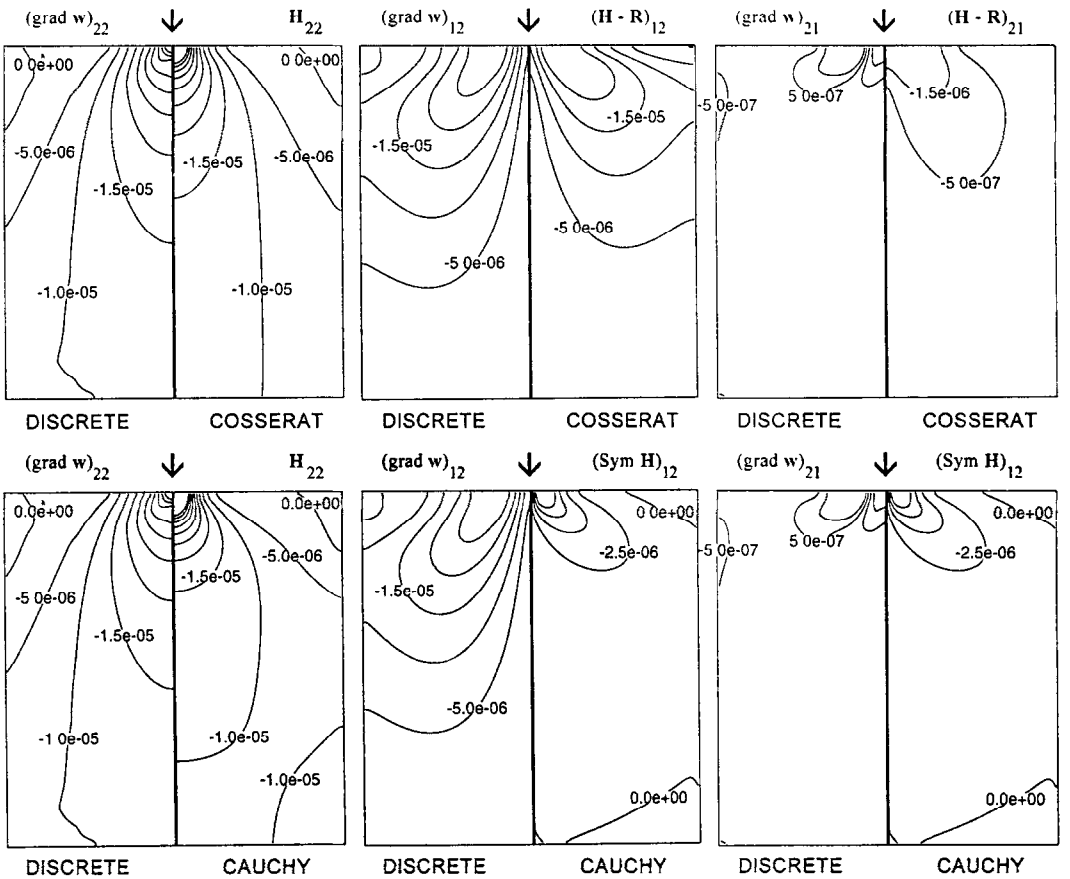

Figure 3. Comparison in terms of strain measures: $(\text{grad } \mathbf{w})_{22}$ to $\mathbf{H}_{22}$, $(\text{grad } \mathbf{w})_{12}$ to $(\mathbf{H}_{12} - \mathbf{R}_{12})$ and $(\text{grad } \mathbf{w})_{21}$ to $(\mathbf{H}_{21} - \mathbf{R}_{21})$.

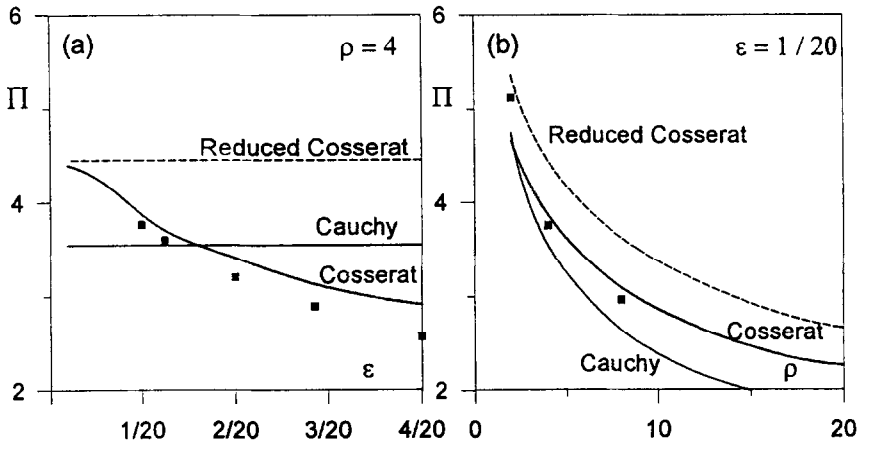

Figure 4. The effects of the size (a) and the aspect (b) parameter. Squares corresponds to the discrete solutions

tetragonal materials, like for example the texture (c) when made of square blocks. This observation has a practical relevance because usually such textures are not used, so that masonries in generally require a micropolar continuous model.

Appendix: Constrained Cosserat Continua

In this section we study the consequences of the two constitutive assumptions introduced in Section 4 (*case C1*): the kinematic constraint (12) and the dynamic restriction on the field of couple stress (10). Since the microrotation and the infinitesimal rigid rotation fields coincide, the linearized strain measure becomes $\mathbf{H} - \mathbf{R} = \operatorname{sym} \mathbf{H}$. Due to the presence of the internal constraint (12), the stress and the couple stress tensors can be divided into the active and the reactive part: $\mathbf{S} = \mathbf{S}^a + \mathbf{S}^r$ and $\mathsf{S} = \mathsf{S}^a + \mathsf{S}^r$. If the constraint is perfect the reactive part is characterized by the condition to spend no power in any admissible strain rate field. Thus, from the power formula for the reactive actions, it follows: $\mathbf{S}^r \in \mathrm{Skw}$ and $\mathsf{S}^r = 0$.

In order to derive the active part of the stress tensor we follow the procedure suggested in [18]. The above kinematical constraint can be regarded as the prescription of a subspace $\mathcal{D}$. This represents the collection of the admissible strain fields

$$\mathcal{D} := \{\mathbf{U} \in \mathrm{Lin} \,|\, \mathbf{U} \cdot \mathbf{V} = 0, \ \forall \mathbf{V} \in \mathrm{Skw}\} \tag{13}$$

which trivially coincides with the subspace of all the symmetric tensors Sym, while its orthogonal complement $\mathcal{D}^\perp$ coincides with Skw. The stress split is such that $\mathbf{S}^a \in \mathcal{D}$ and $\mathbf{S}^r \in \mathcal{D}^\perp$ while S^a and S^r are identically zero. The active part of the stress depends on the admissible strain by a linear map whose symmetric transformations must be compatible with the imposed constraint. Here the symmetry group of the constrained material is $\mathcal{G}_{\check{\mathbb{A}}}$ in (9) and, since the symmetry group of the constraint subspace $\mathcal{D}$

$$\mathcal{G}_{\mathcal{D}} := \{\mathbf{Q} \in \mathrm{SO(3)} \,|\, \mathbf{Q} * \mathbf{U} \cdot \mathbf{V} = 0; \ \forall \mathbf{U} \in \mathcal{D}, \ \forall \mathbf{V} \in \mathcal{D}^\perp\} \tag{14}$$

coincides with the whole group of the proper orthogonal transformations SO(3), the consistency that $\mathcal{G}_{\check{\mathbb{A}}} \subset \mathcal{G}_{\mathcal{D}}$ is always verified. The dynamical constraint (10) entails $\mathbb{C} = 0$; moreover, if the material is hyperelastic, it follows $\mathbb{B} = 0$ and the constitutive equation (7a) becomes $\mathbf{S} = \mathbb{A}[\operatorname{sym}\mathbf{H}]$. The linear map of $\mathcal{D}$ into itself can be deduced by the restriction $-|_{\mathcal{D}}-$ on $\mathcal{D}$ of the constrain-free map $\mathbb{A}$, followed by an orthogonal projection $-\mathbb{P}_{\mathcal{D}}-$ on $\mathcal{D}$. Thus the constitutive relationship for the active part of the stress tensor results[11]

$$\mathbf{S}^a = \mathbb{P}_{\mathcal{D}}\mathbb{A}|_{\mathcal{D}}[\operatorname{sym} \mathsf{H}]. \tag{15}$$

We observe that $\mathbb{P}_{\mathcal{D}}\mathbb{A}|_{\mathcal{D}}$ coincides with the elasticity tensor of the Cauchy equivalent material $\check{\mathbb{A}}$, from Equation (8) and then $\mathbf{S}^a = \check{\mathbf{S}}$.

The reactive part of the stress tensor can be determined from the moment balance equation Equation (13b) in [10] and, by substituting it into the force balance equation, we obtain a 'pure' dynamic equation

$$\operatorname{div}(\mathbf{S}^a + \tfrac{1}{2}\mathbf{B}) + \mathbf{b} = \mathbf{0} \tag{16}$$

which, for $\mathbf{B} = \mathbf{0}$, corresponds to the motion equation for a Cauchy body. The boundary conditions, in terms of external contact force $\mathbf{f}$ and couple $\mathbf{M}$, are $\mathbf{Sn} = \mathbf{f}$ and $\mathbf{M} = \mathbf{0}$. As expected, a compatibility problem arises on the data $\mathbf{M}$. By considering Equations (16) and (15) it is possible to determine directly the displacement field $\mathbf{u}$ from

$$\operatorname{div}(\check{\mathbb{A}}[\operatorname{sym}(\operatorname{grad}\mathbf{u})]) + \mathbf{b} = \mathbf{0}, \tag{17}$$

[11] $\mathbb{A}|_{\mathcal{D}} := \mathcal{D} \to \mathrm{Lin}, \mathbb{P}_{\mathcal{D}} := \mathrm{Lin} \to \mathcal{D}$. In 2-D, $\mathbb{P}_{\mathcal{D}} := \mathbf{I}\boxtimes\mathbf{I} - \frac{1}{2}\mathbf{V}\otimes\mathbf{V}$, $\mathbf{V} = \mathbf{e}_2\otimes\mathbf{e}_1 - \mathbf{e}_1\otimes\mathbf{e}_2$. $(\mathbf{A}\boxtimes\mathbf{B})\mathbf{C} = \mathbf{A}\mathbf{C}\mathbf{B}^T$.

and then the field of microrotation $\mathbf{R} = \text{skw}(\text{grad}\,\mathbf{u})$. Such a material is defined continuum with latent microstructure in [19]. We conclude that by prescribing Equations (12) and (10), for zero density of the mass couple, the material behaves as a Cauchy continuum.

If we consider only the internal constraint (12) we obtain the so-called continuum with constrained rotations [20]. Instead, if we assume the sole position (10) the stress-strain relationship (7a), for the hyperelastic material, becomes $\mathbf{S} = \mathbb{A}[\mathbf{H} - \mathbf{R}]$. The balance equations, in terms of displacement, become

$$\text{div}(\mathbb{A}[\text{grad}\,\mathbf{u} - \mathbf{R}]) + \mathbf{b} = \mathbf{0}, \qquad 2\,\text{skw}(\mathbb{A}[\text{grad}\,\mathbf{u} - \mathbf{R}]) = \mathbf{B} \tag{18}$$

with the above boundary conditions: $\mathbf{Sn} = \mathbf{f}$ and $\mathbf{M} = \mathbf{0}$. If the body density couple is absent, we obtain the material we called reduced Cosserat continuum, whose distinctive feature is to spend zero power with any field of microrotation gradient H. Its stress tensor **S** is a symmetric tensor depending both on the symmetric and the skew-symmetric part of the strain $(\mathbf{H} - \mathbf{R})$.

References

1. Page A. W., 'Finite element model for masonry', *Journal of the Structural Division, ASCE*, **104**(ST8) (1978) 1267–1285.
2. Arya S. and Hegemier G. A., 'Finite element method for interface problems', *Journal of the Structural Division, ASCE*, **108**(ST2) (1982), 327–342.
3. Livesley R. K., 'A computational model for the limit analysis of three-dimensional masonry structures', *Meccanica*, **27**(3)(1992), 161–172.
4. Boothby T. E. 'Stability of masonry piers and arches including sliding', *Journal of Engineering Mechanics, ASCE*, **120**(2)(1994), 304–319.
5. Pietruszczak S. and Niu X., 'A mathematical description of macroscopic behaviour of brick masonry', *International Journal of Solids and Structures*, **29**(5)(1992), 531–546.
6. Alpa G. and Monetto I., 'Microstructural model for dry block masonry walls with in-plane loadings', *Journal of Mechanics and Physics of Solids*, **42**(1994), 1159–1175.
7. Anthoine A., 'Derivation of the in-plane elastic characteristics of masonry through homogenization theory', *International Journal of Solids and Structures*, **32**(2)(1995), 137–163.
8. Besdo D., 'Inelastic behaviour of plain frictionless block-systems described by Cosserat media', *Archives of Mechanics*, **37**(1985), 603–619.
9. Mühlhaus H.-B., 'Application of Cosserat theory in numerical solution of limit load problems', *Ingenieur-Archiv*, **59**(1989), 124–137.
10. Masiani R., Rizzi N. and Trovalusci P., 'Masonry as structured continuum', *Meccanica*, **30**(6)(1995), 673–683.
11. Mühlhaus H. B. and Vardoulakis I., 'The thickness of shear bands in granular materials', *Geotechnique*, **37**(3)(1987), 271–283.
12. Su X. M., 'Strain localization in plane strain micropolar elasticity', *Archive of Applied Mechanics*, **64**(1994), 258–266.
13. Chang S. C. and Liao C., 'Constitutive relation for a particulate medium with the effect of particle rotation', *International Journal of Solids and Structures*, **26**(4)(1990), 437–453.
14. Sternberg E. and Muky R., 'The effect of couple-stresses on the stress concentration around a crack', *International Journal of Solids and Structures*, **3**(1967), 69–95.
15. Bogy D.B. and Sternberg E., 'The effect of couple-stresses on the corner singularity due to an asymmetric shear loading', *International Journal of Solids and Structures*, **4**(1968), 159–174.
16. Trovalusci P. and Masiani R., 'Simmetrie materiali di sistemi discreti e di continui micropolari equivalenti' in *Atti XII Congresso Nazionale AIMETA*, vol. I, Napoli, Italia, 1995, pp. 211–216.
17. Podio-Guidugli P. and Marzano S., 'Materiali elastici approssimativamente vincolati', *Rendiconti Seminari di Matematica Università di Padova*, **73**(1985).
18. Podio-Guidugli P. and Vianello M., 'The representation problem of constrained linear elasticity', *Journal of Elasticity*, **28**(1992), 271–276.
19. Capriz G., *Continua with Microstructure*. Springer-Verlag, Berlin, 1989.
20. Sokolowski M., *Theory of couple-stresses in bodies with constrained rotations*. CISM, Udine, 1972.